$RbGd_2Br_7$:Ce Scintillators for Gamma Ray and Thermal Neutron Detection

Kanai S. Shah, Leonard Cirignano, Ronald Grazioso, Misha Klugerman, Paul R. Bennett, Tapan K. Gupta, William W. Moses, Marvin J. Weber, and Stephen E. Derenzo

***Abstract*-- In this paper, we report on gamma ray and thermal neutron detection with $RbGd_2Br_7$:Ce scintillators. $RbGd_2Br_7$:Ce (RGB) is a new scintillator material, which shows high light output (56,000 photons/MeV) and has a fast principal decay constant (45 ns) when doped with 10% Ce. These properties make RGB an attractive scintillator for γ-ray detection. Also, due to the presence of Gd as a constituent, RGB has a high cross section for thermal neutron absorption and can achieve close to 100% stopping efficiency with 0.5 mm thick RGB crystals. Crystals of RGB with three different Ce concentrations (0.1, 5, and 10%) have been grown and their basic scintillation properties such as light output, decay time, and emission spectrum have been measured. In addition, high efficiency thermal neutron detection has been confirmed in our studies.**

I. Introduction

Scintillation spectrometers are used widely in the detection and spectroscopy of energetic photons (γ-rays) and neutrons at room temperature. These detectors commonly are used in nuclear and high-energy physics research, medical imaging, diffraction, non-destructive testing, nuclear treaty verification and safeguards, and geological exploration [1], [2].

Important requirements for the scintillation crystals used in these applications include high light output, high stopping efficiency, fast response, low cost, good linearity, and minimal afterglow. These requirements cannot be met by any of the commercially available scintillators and there is continued interest in the search for new scintillators with enhanced performance.

Recently, a new cerium doped halide scintillator, $RbGd_2Br_7$:Ce (RGB) has been discovered which has attractive scintillation properties [3], [4]. RGB (with 10% Ce^{3+} doping) has a very high light output (≈56,000 photons/MeV), fast principle-decay constant (43 ns), very good linearity in energy response over a wide energy range, and decent γ-ray detection efficiency [3], [4].

Based on these properties, RGB is very promising for γ-ray spectroscopy. Additionally, this scintillator can be considered for thermal neutron detection due to the presence of Gd as a constituent. One of the isotopes of Gd, ^{157}Gd, has a very high cross section for absorption of thermal neutrons (255,000 b), and the Q value for thermal neutron absorption with ^{157}Gd is also very high (8 MeV). Furthermore, the fast response and high light output of RGB would be beneficial for neutron detection.

In view of the attractive properties of RGB for γ-ray and thermal neutron detection and of the availability of only very small crystals of this material, we have performed an investigation of the crystal growth of this exciting material and have explored its capabilities for γ-ray and neutron detection. In this paper, we report on RGB crystal growth, the evaluation of scintillation properties of RGB with three different Ce concentrations, the characterization of its γ-ray detection properties (such as energy and timing resolution), and thermal neutron detection with RGB.

II. Crystal Growth of RGB

RGB crystals have an orthorhombic structure with a density of 4.7 g/cm^3. The compound melts congruently at 590 °C and, therefore, its crystals can be grown using melt-based methods such as the Bridgman and Czochralski processes. This is fortunate because these melt-based processes are well suited for growth of large volume crystals [5]. In our research, we used the Bridgman method for growing RGB crystals because this technique is easy to implement and quickly can provide good indication of the feasibility of producing large crystals of RGB from the melt.

For the growth of RGB using the Bridgman method, we used a two-zone furnace similar to the one shown in Figure 1. Quartz ampoules were used as crucibles because the melting point of RGB is 590° C, which is substantially lower than the softening point of quartz. Since RGB is not commercially available as a compound, it was synthesized by mixing its constituents (RbBr and $GdBr_3$) in stoichiometric proportions (1:2). We incorporated Ce^{3+} by adding an appropriate amount of $CeBr_3$ to the mixture. Ultra-dry forms of these constituents were purchased from Alfa/Aesar with 99.99% purity. These constituents were mixed and then placed in an evacuated quartz ampoule. The ampoule was heated to a temperature of about 850° C in a tube furnace, which is above the melting point of RbBr (m.p. 693 °C), GdBr3 (m.p. 770 °C) and CeBr3 (m.p. 733 °C). This

Manuscript received Nov. 4, 2001. This work was supported in part by the U.S. Department of Commerce under Grant No. BS123456.

K. Shah, L. Cirignano, R. Grazioso, M. Klugerman, P. Bennett, and T Gupta are with Radiation Monitoring Devices, Inc., Watertown, MA 02472 USA (telephone: 617-926-1167, e-mail: kshah@rmdinc.com, lcirignano@rmdinc.com, rgrazioso@rmdinc.com, mklugerman@rmdinc.com, pbennett@rmdinc.com, and tgupta@rmdinc.com).

W. W. Moses, M. J. Weber, and S. E. Derenzo are with Lawrence Berkeley National Laboratory, Berkeley, CA 94720 USA. (e-mail: wwmoses@lbl.gov, mjweber@lbl.gov, and sederenzo@lbl.gov).

allowed the constituents to mix well and react in the melt phase to form RGB. Upon cooling, the solid phase of RGB formed and was used as a feed material for the Bridgman growth process.

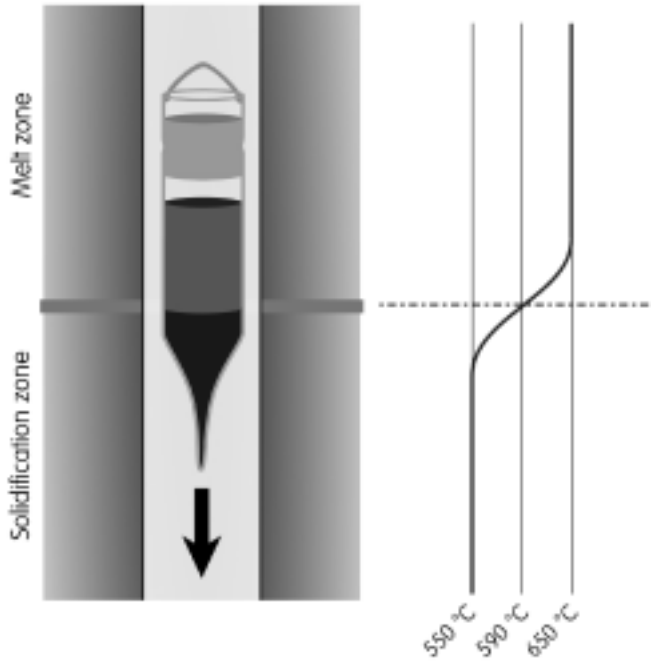

Fig 1. Schematic diagram of the Bridgman setup used for RGB crystal growth.

During the Bridgman growth, the synthesized RGB material was placed in an evacuated quartz ampoule and dropped through a two-zone furnace (shown in Figure 1). The temperature of the upper zone was kept at about 650 °C, while that of the lower zone was about 550 °C. This allowed the growth of the RGB crystal as the ampoule moved gradually from the higher temperature zone to the lower temperature zone. Furthermore, the temperature of 550 °C in the cooler zone provided annealing of the crystal before it cooled to room temperature. The growth rate (or the dropping rate for the ampoule) was an important process parameter in our study. The dropping rate of the ampoule determines how close the conditions at the solid-liquid interface come to equilibrium. At very slow rates, the system operates close to equilibrium. Typical growth rates for the Bridgman process are 1-10 mm/hr, however, certain layered structures require slower rates. We used a growth rate of about 5 mm/day in our research. Most growth runs were performed with 10% cerium concentration, although some runs were also performed with lower Ce^{3+} concentration (0.1% and 5%) in order to study the effect of variation in cerium concentration on the scintillation properties of this material.

A photograph of one RGB crystal removed from the growth ampoule is shown in Figure 2. We found that the boules had large sections which were of single crystal orientation (1-2 cm^3). In many cases, the crystals that separated along cleavage planes were very transparent and the exposed faces had a smooth appearance. In such cases, no polishing of the crystals was required. In other cases, the exposed faces were polished using non-aqueous slurries (due to the hygroscopic nature of RGB) prepared by mixing mineral oil with Al_2O_3 grit.

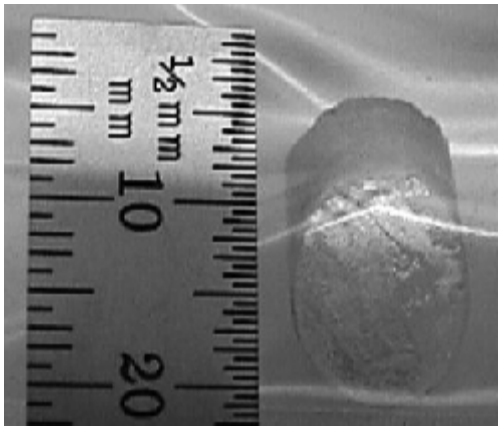

Fig. 2 Photograph of a RGB crystal, freshly removed from a growth ampoule.

These crystals were then packaged to prevent exposure to moisture. This involved encapsulating the crystal in an epoxy (EPO-TEK epoxy 301-2) with a thin, quartz window (0.5 mm) placed on the crystal face which would be coupled to an optical sensor.

III. Scintillation Properties of RGB

We have characterized some of the scintillation properties of RGB crystals grown by the Bridgman process. This investigation involved the measurement of its light output, emission spectrum, and fluorescent decay time of RGB samples. The variation of these scintillation properties with Ce^{3+} concentration was analyzed.

A. Light Output Measurements

The light output of RGB crystals was measured by comparing their response to 662 keV γ-rays (^{137}Cs source) to the response of calibrated LSO and CsI(Tl). These measurements involved optical coupling of an RGB crystal to a photomultiplier tube (PMT) (with a multi-alkali S-20 photocathode), irradiating the scintillator with 662 keV photons, and recording the resulting pulse height spectrum. In order to maximize the light collection, the packaged RGB crystals were wrapped in a reflective, white Teflon tape on all faces (except the one coupled to the PMT). Silicone fluid was applied at the PMT-scintillator interface. The PMT output was connected to a preamplifier (Canberra 2005) and the preamplifier output was amplified and shaped with a spectroscopy amplifier (Canberra 2020). A pulse height spectrum was recorded with an amplifier shaping time of 2.0 μs with an RGB crystal (10% Ce doping). This experiment was then repeated with a calibrated LSO scintillator having a light output of 21,000 photons/MeV as shown in Figure 3. A comparison of the photopeak position obtained with RGB for 662 keV photon energy to that with LSO provided an

estimation of the light output for RGB crystals. The packaging of the RGB crystals used for light output studies was not optimized for energy resolution measurements.

Since the peak emission wavelength is similar for LSO and RGB, no correction was performed for differences in quantum efficiency of the photocathode. Based on the recorded photopeak positions shown in Figure 3 for RGB and LSO, we estimated the light output of RGB crystal with 10% Ce to be about 57,000 photons/MeV at a shaping time of 2 μs.

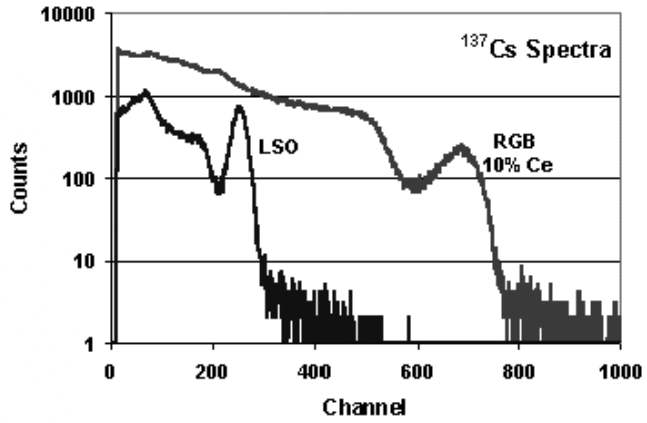

Figure 3. ^{137}Cs spectra recorded with RGB (10% Ce) and LSO crystals coupled to a PMT under identical conditions. The light output of RGB (10% Ce) was estimated to be 57000 photons/MeV from the calibration provided by LSO.

We also studied the variation in light output of RGB crystals as a function of the cerium concentration in the crystals. Crystals with cerium concentrations of 0.1%, 5%, and 10% were investigated. Each crystal was coupled to a PMT and 60 keV γ-ray spectra (^{241}Am) were recorded with these crystals under identical operating conditions (see Figure 4). A shaping time of 2 μs was used. As seen in the figure, the light output of RGB clearly increases as the Ce concentration increases. The estimated values of light output for all three Ce concentrations are listed in Table I.

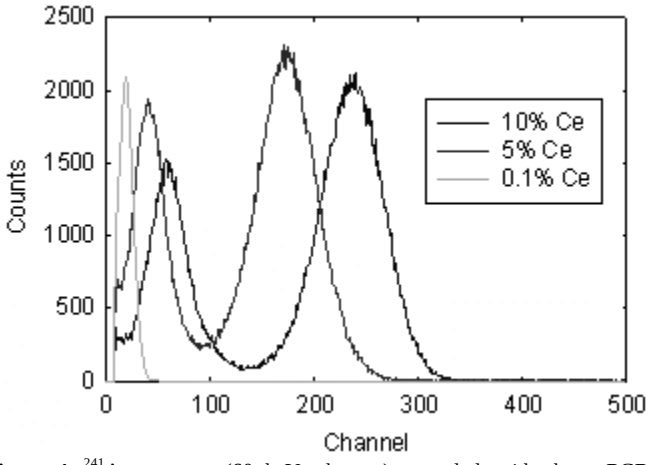

Figure 4. ^{241}Am spectra (60 keV photons) recorded with three RGB crystals having different Ce concentration. From the peak position, light output was estimated for each crystal.

B. Emission Spectrum

We have measured the emission spectra of the RGB scintillators. The RGB samples were excited with radiation from a Philips X-ray tube having a copper target, with power settings of 30 kVp and 15 mA. The scintillation light was passed through a monochromator and detected by a PMT (Hamamatsu C31034) with a quartz window. The system was calibrated with a standard light source to enable correction for sensitivity variations as a function of wavelength. The measured emission spectra for a RGB sample with 10% Ce concentration is shown in Figure 5. As seen in the figure, the emission peak is at about 430 nm which is similar to the results reported earlier [3]. Emission measurements were performed for RGB samples with 0.1% and 5% Ce concentration with similar results.

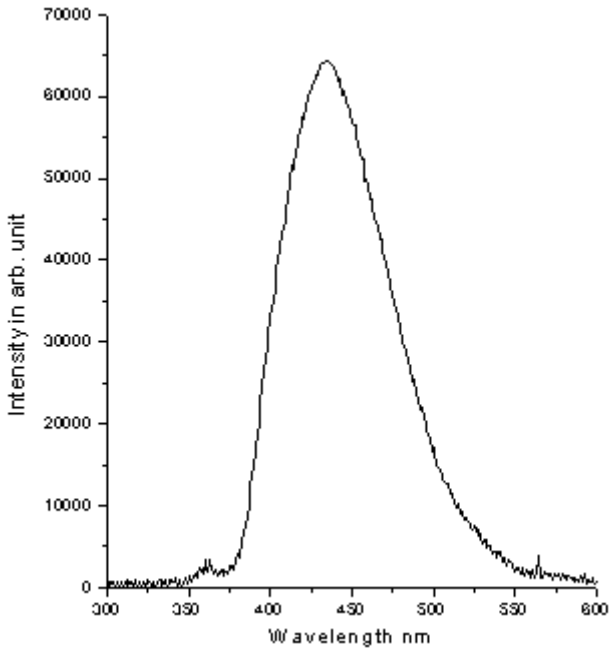

Figure 5. RGB (10% Ce) emission spectrum.

C. Decay Time

The fluorescent decay time of RGB crystals (with 0.1, 5, and 10% Ce) was measured using the delayed coincidence method [6] at Lawrence Berkeley National Laboratory (LBNL). Decay time measurements were made using the LBNL Pulsed X-Ray Facility. The X-ray source is a light-excited X-ray tube that produces 4,000 X-ray photons (mean energy 18.5 keV) per steradian in each 1 ps FWHM pulse with a 50 kHz repetition rate. The RGB samples were placed in the X-ray beam and their fluorescent emanations were detected with a sapphire-windowed microchannel plate PMT (spectral range 150-650 nm, transit time jitter 40 ps FWHM). The time difference between the X-ray pulse and the detected fluorescent emissions was measured using a time-to-amplitude converter / analog-to-digital converter combination having 2 ps FWHM resolution. The decay time spectrum was acquired with the delayed coincidence method [6]. The total system response time is 60 ps FWHM.

TABLE I. SCINTILLATION PROPERTIES OF RGB WITH DIFFERENT CE CONCENTRATIONS

Ce^{3+} Concentration [%]	Light Output [photons/MeV]	Decay Time(s) [ns]	Emission Peak [nm]
0.1	4,400	3 (13.6%), 60 (66.3%), 400 (20.1%)	430
5	42,000	50 (91%), 400 (9%)	430
10	57,000	45 (53%), 400 (47%)	430

The decay time spectrum for each RGB sample was fit to the sum of exponential decay times, with up to three exponential decay components, and a time-independent background at LBNL. The results are shown in Figure 6, and all three samples show very fast principal decay constants (45-60 ns). The results of the light output, emission spectrum, and decay time measurements for three different Ce concentrations are listed in Table I. As seen in Table I, RGB with 10% Ce^{3+} concentration shows a high light output and fast principal decay constant. The parameter – photons/(ns-MeV), which is a figure of merit for timing applications, is about 800 for RGB (10% Ce). This value is higher than that in all established inorganic scintillators with exception of BaF_2.

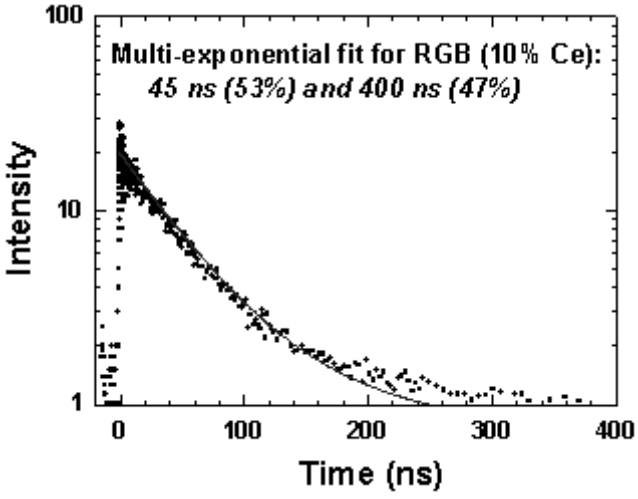

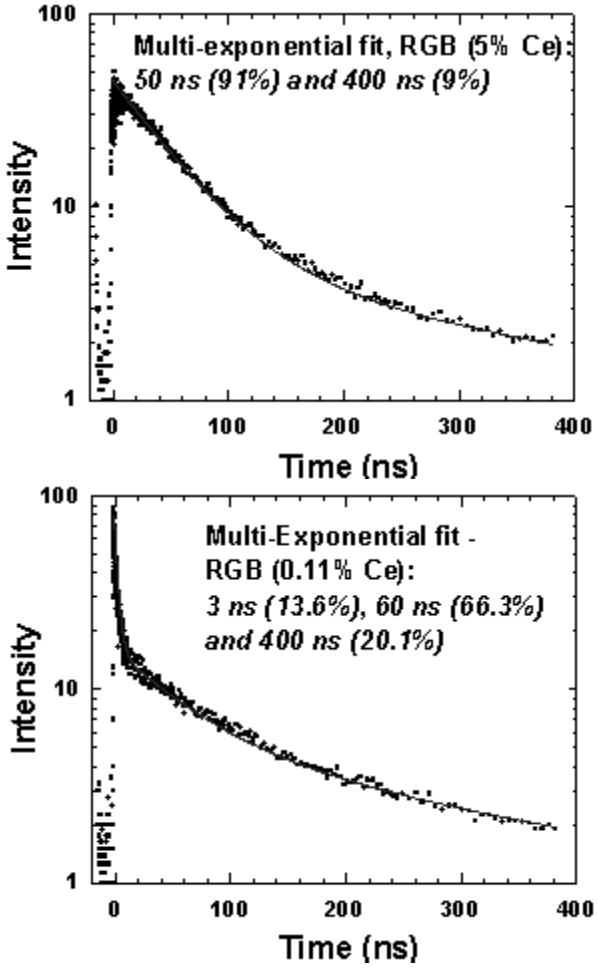

Figure 6. Decay time spectra for RGB crystals with 0.1, 5, and 10% Ce^{3+} concentration measured using a pulsed X-ray source at LBNL, along with multi-exponential fits to the measured data. The principal decay constant is fast (≤ 60 ns) for all three samples. Different X-ray exposures were used for each sample.

D. Energy and Timing Resolution

We measured the γ-ray energy resolution of the RGB scintillators. This involved coupling an unpackaged RGB scintillator (10% Ce) to a PMT with a multi-alkali S-20 photocathode. The scintillator was coated with Teflon tape to maximize the light collection. The scintillator was irradiated with 662 keV γ-rays (^{137}Cs source), the PMT signal was processed with a preamplifier (Canberra #2005), and then the signal was shaped with a spectroscopy amplifier (Canberra #2020). A ^{137}Cs pulse height spectrum was recorded with shaping time of 0.5 μs, as shown in Figure 7, and the energy resolution for the 662 keV peak was computed to be about 5.2% (FWHM) at room temperature.

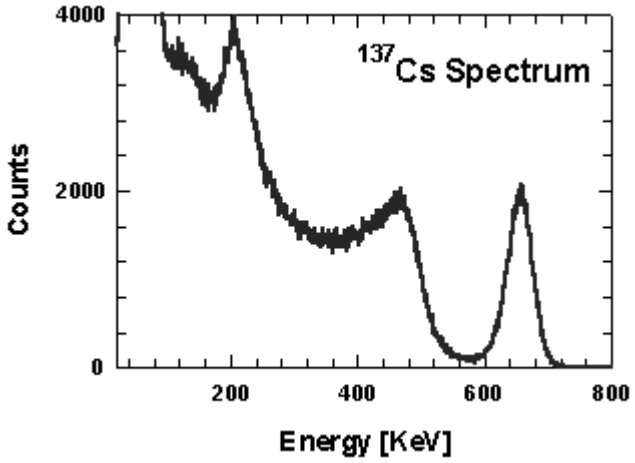

Figure 7. A ^{137}Cs spectrum recorded with an RGB scintillator coupled to a PMT at room temperature.

The coincidence timing resolution of an RGB crystal was measured at LBNL. This experiment involved irradiating a BaF_2 and an RGB scintillator (each coupled to a fast PMT) in a coincidence setup with 511 keV positron annihilation γ-ray pair (emitted by a ^{22}Na source). The BaF_2-PMT detector formed a "start" channel in the timing circuit, while the RGB-PMT detector formed the stop channel. The time difference between the two channels with fixed delay between them was observed in a timing spectrum recorded on an MCA (see Figure 8). The coincidence timing resolution was measured to be 330 ps (FWHM). Similar coincidence studies with two BaF_2 samples (one in the start and the other in the stop channel) produced a coincidence-timing resolution of 273 ps (FWHM). Thus, the timing resolution of one RGB sample would be 267 ps and of two RGB samples in coincidence would be 374 ps (FWHM).

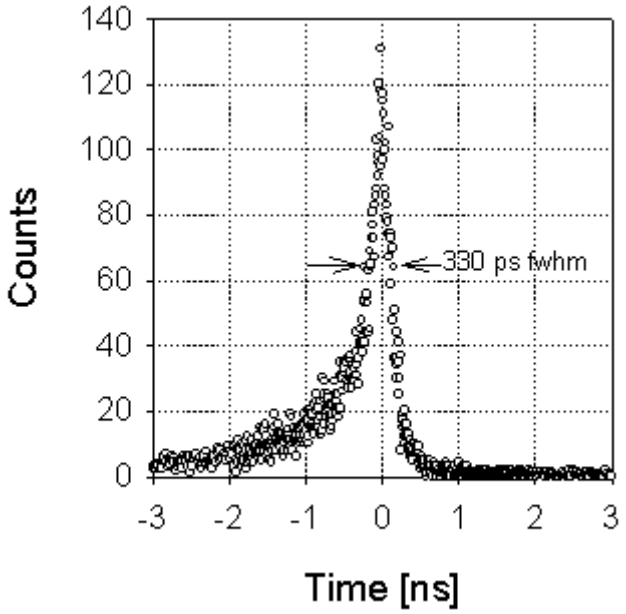

Figure 8. The coincidence timing resolution with RGB-PMT and BaF2-PMT detectors irradiated with 511 keV γ-ray pair. The FWHM of the peak is 330 ps.

IV. Thermal Neutron Detection

In addition to γ-ray detection, RGB can function as a thermal neutron detector due to the presence of Gd as one of the constituents. Two isotopes of Gd, ^{157}Gd and ^{155}Gd, have very high thermal neutron absorption cross-sections of about 2.55 x 10^5 b and 6.1 x 10^4 b, respectively. About 80% of the neutron capture events in Gd occur in ^{157}Gd and about 18% occur in ^{155}Gd [7]. Due to the high thermal neutron cross section of ^{157}Gd (255,000 b), RGB layers with 200 μm thickness can provide ~90% stopping efficiency for thermal neutrons, while the stopping efficiency for 500 μm RGB layers is close to 100%. Such a small thickness requirement for thermal neutrons is helpful in minimizing the γ-ray background effects.

Upon absorption of thermal neutrons with Gd, ^{158}Gd and ^{156}Gd are formed, and the excitation energy is given up through a cascade of high-energy γ-rays. Furthermore, the de-excitation of ^{158}Gd and ^{156}Gd passes through low level states where internal conversion occurs and conversion electrons and low energy X-rays are released. Thus, the reaction products for neutron capture with Gd are γ-rays, low energy X-rays, and conversion electrons [7]. In many instances, these conversion electrons and low energy X-rays form the basis of neutron detection.

Overall, in 87% of all thermal neutron capture events in Gd, conversion electrons in a 29 to 182 keV range are released [8]. In the case of ^{158}Gd, the final $2^+ \rightarrow 0^+$ transition generates conversion electrons in the 29.3 to 77.7 keV range from the K-shell to the M-shell, respectively [9]. The K-shell binding energy is 50.2 keV which results in a 29.3 keV conversion electron. The three L-shell binding energies are 8.3, 7.9, and 7.2 keV for the L_I, L_{II}, and L_{III} shells, respectively. These would result in conversion electrons of ~72 keV for all three L-shells. The M-shell binding energy is 1.8 keV, which would result in a 77.7 keV conversion electron. Thus, in the case of scintillation based detectors, two peaks, one at about 29 keV and the other at about 72 keV can be used to register neutron detection. The final $2^+ \rightarrow 0^+$ transition in the case of ^{156}Gd is similar, with the conversion electron energies slightly higher. Since scintillation crystals are not able to distinguish emissions from these two isotopes, the energy of peaks resulting from thermal neutron reaction are ~34 keV and ~74 keV [7]. Both these peaks can be utilized to confirm thermal neutron detection with Gd based detectors such as GSO or RGB [7].

The K-shell conversion electron emission occurs in 26% of all thermal neutron capture reactions with Gd and is accompanied by a 44 keV K-shell X-ray. The X-ray escapes in about 50% of cases because thermal neutron absorption in Gd-based detectors occurs near the surface [7]. Thus, about 13% of all thermal neutron capture events are present in the lower 34 keV peak. In the other 50% of K-shell associated events, the conversion electron and X-ray energies are absorbed together and an event with 78 keV energy is recorded. As mentioned earlier, the 74 keV peak is mostly

due to conversion electron emission from the L- and M-shells, which occurs for 40% of all thermal neutron reactions with Gd. Furthermore, the combined energy of K-shell conversion electron and Gd K-shell X-ray events (which occur for 13% of all neutron capture events in Gd) is ~78 keV which are also present in the higher energy peak. Thus, the 74 keV peak represents 53% of all Gd-based thermal neutron capture events, and the sum of 34 and 74 keV peaks represents 66% of the neutrons captured by Gd. If full integration of the conversion electron spectrum from 29 to 182 keV were performed, 87% of the events would be covered.

In our studies, a 1 mm thick RGB crystal (1 cm^2 area, with 10% Ce) was coupled to a PMT and irradiated with thermal neutrons from a moderated ^{252}Cf source. The source was placed in a lead enclosure and was surrounded by a cylindrical polyethylene shell. The lead enclosure was 1.25 cm thick and the polyethylene shell was 6.0 cm thick. The polyethylene shell moderated a large majority of the neutrons to thermal energies (~0.0253eV). A 1/8" thick copper plate was placed between the scintillator and the source to reduce any gamma or X-ray interactions in the RGB crystal. In this arrangement, energy deposited due to gamma ray interactions in RGB is minimal because most of the gamma rays are stopped by the lead enclosure or the copper plate. Therefore, we expected to see the neutron induced peaks at 34 and 74 keV sitting on top of a small background curve, which was indeed observed in our experiments as shown in Figure 9 (see the spectrum labeled "source").

A background spectrum was also acquired by placing two sheets of ^{10}B-loaded rubber (1/8" thick) between the source chamber and RGB detector. The boron sheets were sufficiently thick to capture almost all thermal neutrons exiting the polyethylene cylinder. The data collected with boron sheets represented the background effects. When boron sheets were placed between the source and RGB crystal, the peaks at 74 keV and 34 keV disappeared, as expected (see the spectrum labeled "background" in Figure 9). This ensured that other effects, such as Pb X-ray emission from the lead enclosure was not responsible for presence of 74 keV peak. This is because 90% of 80 keV Pb X-rays would easily pass through two ^{10}B- rubber sheets, and would therefore, appear in the spectrum, which is not the case. This confirmed that the 34 and 74 keV peaks seen in Figure 9 are due to thermal neutron capture reaction with Gd in RGB. The background counts are mostly due to self-emission of RGB (from beta decay of ^{87}Rb) which can be seen in the spectrum acquired without the ^{252}Cf source placed in front of the detector, which is shown in Figure 9 with label "no source (decay of Rb-87)".

Based on the calibration of thermal neutron emission from our ^{252}Cf source, we estimate the efficiency of the RGB detector to be ~60% based on integration of counts in the 34 and 74 keV peaks. Even higher efficiency (~87%) can be obtained by integration of all conversion electron events between 29 and 182 keV, which will be explored in our future research.

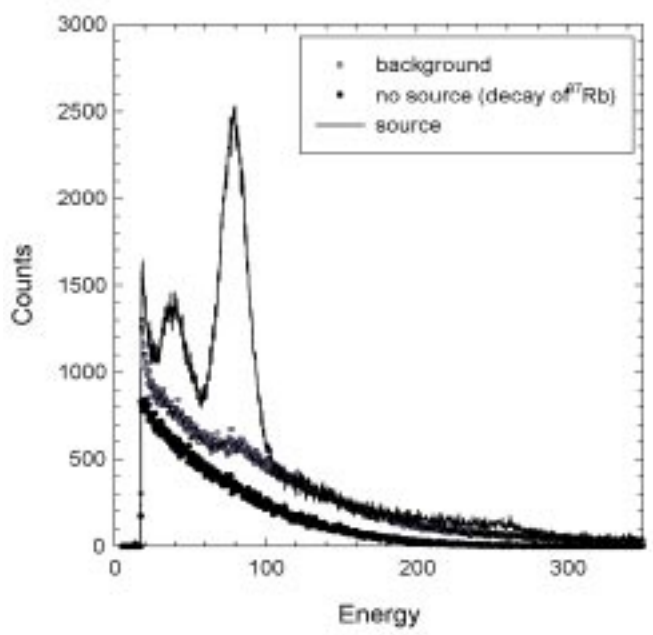

Figure 9. Energy spectra with RGB (using ^{252}Cf source) showing 34 and 74 keV peaks, characteristic for thermal neutron interaction with Gd (labeled "source"), a "background" spectrum (recorded with two sheets of ^{10}B rubber placed between the source and the RGB detector), and a spectrum showing intrinsic counts in RGB without any source due to β-decay of ^{87}Rb (labeled "no source").

V. Summary

In our research, we have investigated a new scintillation material, $RbGd_2Br_7$:Ce, for gamma ray and neutron detection. Our research concentrated on growth of high quality $RbGd_2Br_7$:Ce crystals using the Bridgman method, as well as extensive characterization of the physical, optical, and scintillation properties of these crystals. Gamma ray and neutron detection capabilities of the new scintillation material were also explored. Based on the successful performance of RGB as a gamma ray and neutron detector, this new scintillation material can be applied to applications such as medical imaging, nuclear physics, X-ray and neutron diffraction, nondestructive evaluation, treaty verification and safeguards, environmental monitoring, and geological exploration.

VI. References

[1] G. F. Knoll, *Radiation Detection and Measurement*, 3rd ed., New York: John Wiley and Sons, 1999.

[2] K. Kleinknecht, *Detectors for Particle Radiation*, 2nd ed., Cambridge, U.K.: Cambridge University Press, 1998.

[3] O. Guillot-Noel et al., "Scintillation properties of RbGd2Br7:Ce advantages and limitations," *IEEE Trans. Nucl. Sci.*, vol. 46, no.5, pp. 1999.

[4] P. Dorenbos et al., "Scintillation properties of RbGd2Br7:Ce crystals; fast, efficient, and high density scintillators," *Nucl. Instr. Meth in Phys.* Res., B132, o. 728, 1997.

[5] J.C. Brice, *Crystal Growth Processes*, UK: Blackie Halsted Press, 1986.

[6] L. M. Bollinger and G. E. Thomas, "Measurement of the time dependence of scintillation intensity by a delayed-coincidence method," *Rev. Sci. Instr.*, vol. 32, pp. 1044, 1961.

[7] P.L. Reeder, “Thin GSO scintillator for neutron detection,” *Nucl. Instr. Meth. in Phys.* Res., A353, pp. 134-136, 1994.
[8] B. Gebauer et al., *Nucl. Instr. Meth*., A392, p. 68, 1997.
[9] R.C. Greenwood et al., “Collective and two-quasiparticle states in ^{158}Gd observed through study of radiative neutron capture in ^{157}Gd,” *Nuclear Physics*, A304, p. 327, 1978.